

Received September 7, 2018, accepted October 6, 2018, date of publication October 17, 2018, date of current version November 14, 2018.

Digital Object Identifier 10.1109/ACCESS.2018.2876505

Simplified Indirect Model Predictive Control Method for a Modular Multilevel Converter

MINH HOANG NGUYEN AND SANGSHIN KWAK^{ID}, (Member, IEEE)

School of Electrical and Electronics Engineering, Chung-Ang University, Seoul 156-756, South Korea

Corresponding author: Sangshin Kwak (sskwak@cau.ac.kr)

This work was supported in part by the National Research Foundation of Korea funded by the South Korean Government (MSIP) under Grant 2017R1A2B4011444 and in part by the Human Resources Development of the Korea Institute of Energy Technology Evaluation and Planning funded by the South Korean Government Ministry of Trade, Industry and Energy under Grant 20174030201810.

ABSTRACT Demand for modular multilevel converters (MMCs) has been steadily increasing for utilization in medium- to high-power applications because of qualities such as high modularity, easy scalability, and superior harmonic performance. Furthermore, there has been a growing trend toward utilizing model predictive control for MMCs due to its simplicity, good dynamic response, and ease of multi-objective control. However, the rise in computational load leads to a great drawback when increasing the number of submodules (SMs). This paper presents an approach to reducing the computational load and using on-state SMs and circulating currents, by preselecting the number of SMs inserted in the upper and lower arms. This approach is based on using the number of on-state SMs and the circulating current, to compute the number of SMs inserted in the upper and lower arms, which is evaluated in the next sampling instant. This facilitates a significant reduction in the number of control options and the computational load. A sorting algorithm is used to retain the balancing capacitor voltages in each SM, while the cost function guarantees the regulation of the ac-side currents, arm voltages, and MMC circulating currents. Simulation and experiment results validate the performance of the proposed approach.

INDEX TERMS Model predictive control (MPC), modular multilevel converter (MMC), circulating current, computational load, preselection.

I. INTRODUCTION

The MMC structure has modularity and scalability, which allows it to synthesize any voltage level, compared to other multilevel converter topologies. As a voltage source converter, owing to the cascaded SMs structure, the MMC can provide output voltage and current waveforms having an excellent harmonic spectrum, which results in sinusoidal voltage waveforms, even without any output filters. Of the two types of output voltage level of the MMC, the maximum phase voltage of the MMC (i.e., $2N + 1$, where N is the number of submodules in the upper or lower arm of each phase) has many advantages compared to $N + 1$, such as considerable suppression of both the ac output harmonics and EMI noise (caused by dv/dt). Owing to these advantages, it has gained attention for use in high-voltage applications for situations where there are a high number of submodules.

In contrast to the $N + 1$ output voltage level, the number of SMs inserted in the one phase (number of on-state SMs in the one phase) of $2N + 1$ output voltage level is not equal to N . The other combinations of the number of

inserted SMs allow it to generate intermediate output voltage levels, and increase the number of output voltage levels in the final waveform [2]. Relationships between the output voltage levels and the number of on-state SMs in one phase are analyzed for a back-to-back MMC configuration for HVDC applications, using two different multi-carrier sinusoidal pulse width modulation (SPWM) methods [2]. Additionally, PWM methods including the carrier-phase-shifted PWM (CPSPWM), level-shifted-PWM (LSPWM) [3], [4], and the improved submodule unified PWM (SUPWM) [5], can also generate output voltage waveforms with $2N + 1$ levels. Compared to the PWM methods, the main advantage of model predictive control (MPC) is that it allows the consideration of a variety of control objectives, by proper selection of the cost function. It also helps to directly control multiple system variables simultaneously, reducing the system's overshoot, and suppressing the nonlinear effect of the converter. Therefore, MPC methods have been widely utilized in the area of power electronics. As for the MPC methods, several control schemes were presented for the MMC [6]–[8].

A finite-control set (FCS) MPC strategy for controlling the output current tracking of the MMC for two distinct cases, balanced reference current and unbalanced reference current, was presented and verified by simulation studies [9]. In [10], the FCS-MPC strategy, the most suitable combination option is chosen by considering N combinations in $2N$ options, i.e., C_{2N}^N in each phase within each sampling period. However, this leads to a sharp increase in the number of control options, as the number of SMs rises, making the implementation of a FCS-MPC strategy impractical due to the major issue of calculation load.

The direct FCS-MPC strategy [11] evaluates 2^{2N} switching states in every sample period to find out optimal switching states. Although this algorithm is easy to realize with straightforward approach, the number of control options and corresponding computation load increase exponentially with the increasing number of the SMs in the MMCs, which makes it difficult to be implemented in a large-scale MMC systems. As a result, several studies have been presented on literature focusing on the reduction of computational load. An approach in [12] proposed an algorithm that utilizes three independent cost functions to control ac output currents, circulating currents, and SM capacitor voltages to select the most suitable switching states. This method can reduce the number of switching states in individual cost function. An indirect FCS-MPC strategy was addressed to decouple the control of SM capacitor voltages from the cost function by utilizing a voltage sorting algorithm [13]. This algorithm determines the number of submodules inserted to the upper arm and the lower arm, respectively, whereas a capacitor voltage sorting algorithm balances SMs capacitor voltages. Because there are $N + 1$ possibilities for the number of output voltage level in each arm, there are $(N + 1)^2$ control options in this FCS-MPC strategy for $2N + 1$ output voltage levels. Compared to the direct FCS-MPC method [11], the indirect FCS-MPC algorithm substantially reduces the computational burden. However, the number of control option is still high when the MMCs with a large number of SMs are considered. An improved MPC was proposed, by changing the number of on-state SMs in one phase based on the voltage level and using the tolerance band of capacitor voltage [14], which allows a reduction of the control option. Fast MPC (FMPC) method, based on the indirect FCS-MPC, was proposed to utilize the nearest levels corresponding to the last output voltage level of the MMC to reduce the number of control option to only two or three [15]. This method selects an appropriate output voltage level, on a basis of an exact look-up table consisting of all possible number of inserted SMs. This algorithm can substantially reduce the number of control options for the MMCs with $N + 1$ output voltage levels. However, there has not been in detail addressed for the MMCs with $2N + 1$ output voltage level. In addition, the complexity issues and the circulating current controllability at high number of SMs in case of $2N + 1$ output voltage level has not been analyzed. A reduction approach for the MMCs with $2N + 1$ output voltage level was proposed using a preselection

algorithm to reduce the number of control option every sampling instant [20]. This method, based on relationships between output voltage levels at a present step and nearest output voltage levels at a next step, preselect the number of inserted SMs to be evaluating at a next sampling instant.

This paper proposes a simple approach to reduce calculation complexity with preselection algorithm by utilizing a redundant number of on-state SMs and its effect on circulating currents, for the MMCs generating the $2N + 1$ output voltage levels. The developed method can preselect the number of inserted SMs in upper arm and lower arm for control options every sampling instant, which is combined in the MPC method. The proposed approach, based on the nearest output voltage level around the last output voltage combined with redundant number of on-state SMs, can preselect the number of inserted SMs, which should be evaluated in the next sampling instant. As a result, the proposed algorithm does not need to evaluate all possible switching state as the indirect FCS-MPC methods, which can allow reduce the number of control options every sampling instant resulting in reduced computational burden [13]. Moreover, the proposed scheme can reduce the number of control option without using individual cost functions as well as with no capacitor voltage tolerance band [12]–[14], which can lead to straightforward implementation. In addition, the proposed method does not need a look-up table, in contrast to the FMPC method, because the proposed algorithm at every sampling instant preselects the number of SMs that should be inserted at a next sampling period [15]. Especially, as for the MMC with a large number of SMs, the proposed method can guarantee the circulating current controllability with less complexity, by increasing the number of control option. Based on redundant number of on-state SMs and its effect on circulating currents, the proposed method can decrease the control options by almost half in comparison with the previous approach in [20]. Thus, the proposed approach can improve computational loads of the MPC by reducing the number of control options, ensuring three crucial controlling objectives of the MMC: correction of sinusoidal form, magnitude of output current or voltage, suppression of circulating current inside the converter, and voltage balancing the capacitors of the submodules. The performance of the proposed method is verified with simulation and experiment results.

This paper is structured as follows: in Section II, the basic structure and operation of the MMC and the conventional MPC strategy are presented; in Section III, the details of the proposed preselected number of SMs inserted in the MPC strategy are presented; in Section IV, the simulation results are presented; in Section V, the results of the experiment are presented; finally, in Section VI, the conclusions are presented.

II. OPERATION OF THE MMC AND CONVENTIONAL MPC STRATEGY

Fig. 1 depicts the typical configuration of a three-phase MMC [1], [16], [17] which contains two arms forming one

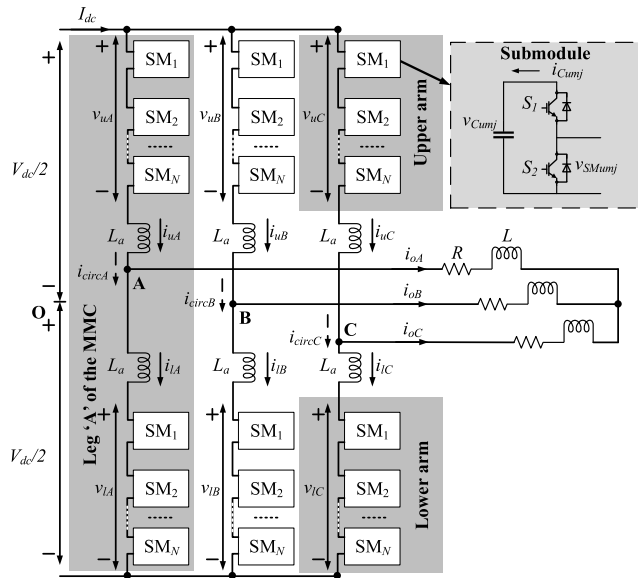


FIGURE 1. Circuit diagram of MMC.

converter phase. An inductor L_a is connected in series with each arm to limit the current due to instantaneous voltage differences of the arms. Each arm is comprised of N SMs, which are the most basic cells of MMCs. The half-bridge cells can generate only zero and positive voltages, corresponding to the switching states of the switches S_1 and S_2 .

A. OPERATION OF MMC

In this study, assuming that the capacitor voltages are charged to their nominal value (V_{dc}/N) for correct operation of the MMC. When all the capacitors are charged to that nominal value the controller then transmits the switching state signal to the SMs to generate the output voltage. The SMs, as illustrated in Fig. 1, can be switched in two different ways: “inserted” state, defined as when S_1 gets switching state ON and S_2 gets switching state OFF, and “bypassed” state, defined as when S_1 gets switching state OFF and S_2 gets switching state ON. Therefore, the phase- j output voltage of the converter $v_{j0}(j = A, B, C)$ can vary between $-V_{dc}/2$ and $V_{dc}/2$, with a maximum of $2N + 1$ voltage levels. When the MMC operates, it requires three control objectives that need to be satisfied for proper operation [1]. The first requirement is the proper magnitude, frequency, and phase of the output currents and voltages. The second requirement is the minimization of circulating current, which is generated due to the unbalanced voltages between the upper and lower arm of the phase leg. The third requirement is the balancing of the capacitor voltages. The SMs capacitor voltages should remain as close as possible to their nominal values of V_{dc}/N .

B. CONVENTIONAL MPC STRATEGY

Fig. 2 (a) illustrates a block diagram of the direct MPC algorithm for MMC, which includes the following steps [17]:

- 1) Predicting one-step forward behavior of the control variables based on a discrete-time model of the system.

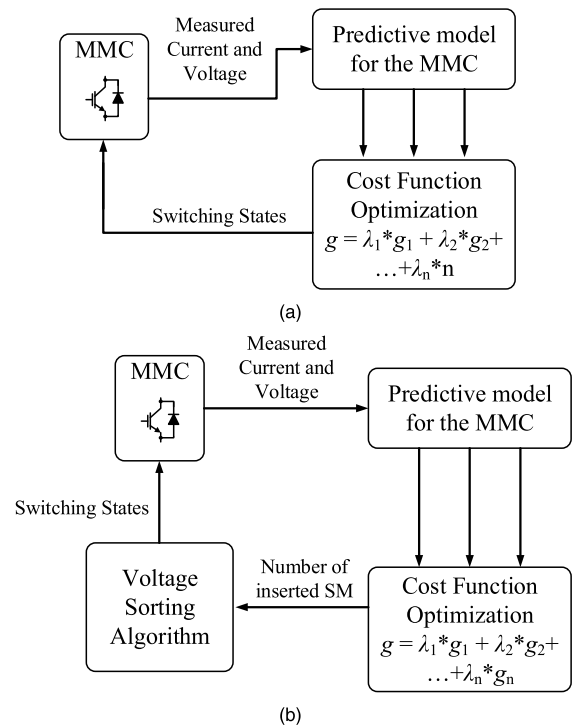


FIGURE 2. Conventional predictive control schemes for MMC (a) direct FCS-MPC (b) indirect FCS-MPC.

- 2) Designing a cost function which describes the desired behavior of the control objectives in the system.
- 3) Evaluating all possible switching states of the MMC through the defined cost function to select the optimal switching state that corresponds to the minimum value of the cost function.

Different from the direct FCS-MPC method, the indirect FCS-MPC, as shown in Fig. 2 (b), decouples SM capacitor voltage balancing from the cost function by using a voltage sorting algorithm. Instead of evaluating all possible switching states, MPC block of the indirect FCS-MPC method determine the number of inserted SMs in the upper and the lower arm. Then, the voltage sorting algorithm block can define which SM inserted or bypass to send the switching state pulses to MMCs and balance the SM capacitor voltages at the same time.

III. PROPOSED MPC STRATEGY FOR MMC

The proposed MPC strategy of using a preselected number of inserted SMs combines the merits of a conventional MPC and the algorithm of retaining SM capacitor voltage balancing based on a voltage sorting method [15]. The proposed strategy will also reduce the computational load. Fig. 3 shows a block diagram of the proposed method. Here: the predictive part predicts the change in the controlled objectives based on a discrete-model of the system; the cost function minimization defines the desired behavior of the system to select the optimal number of SMs inserted in the upper and lower arms (n_{uj}, n_{lj}) that results in the optimal value for the cost function;

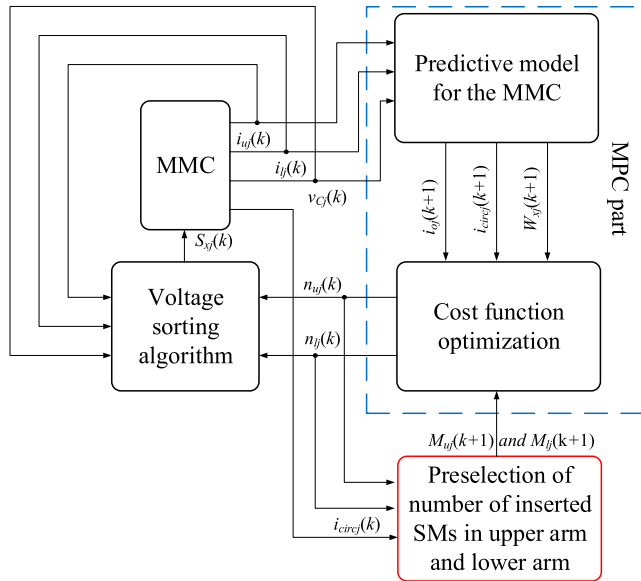


FIGURE 3. Block diagram of the proposed MPC strategy based on preselection algorithm.

the preselection block generates the predicted number of SMs to be inserted in the upper and lower arms (M_{uj} , M_{lj}) to be evaluated in the next sampling instant; and the capacitor voltage sorting block keeps the SMs capacitor voltages balanced, and generates the switching signals.

A. OUTPUT CURRENT CONTROL

As depicted in Fig. 1, the ac-side output current of phase- j can be described as

$$i_{oj} = i_{uj} - i_{lj} \tag{1}$$

where, i_{uj} and i_{lj} are the upper and lower arm currents, respectively. One of the control objectives is to control the output current of the MMC. From (1) and [16], the mathematical equation of the output current is expressed as

$$\frac{di_{oj}}{dt} = \left(\frac{1}{2L + L_a} \right) (v_{lj} - v_{uj} - 2Ri_{oj} - 2v_{com}) \tag{2}$$

where, v_{uj} and v_{lj} are the upper and lower arm voltages, respectively, and v_{com} is the common mode voltage of the MMC. As an MPC operates in the discrete-time domain, the mathematical model of the output current can be obtained by utilizing the Euler approximation for the current derivative, presented as [18]:

$$i_{oj}(k + 1) = \left(\frac{T_{sp}}{2L + L_a} \right) (v_{lj}(k) - v_{uj}(k)) + \left(1 - \frac{2RT_{sp}}{2L + L_a} \right) i_{oj}(k) - T_{sp} \frac{2v_{com}}{2L + L_a} \tag{3}$$

where, $i_{oj}(k + 1)$ and $i_{oj}(k)$ are the predicted output current and measured output current, respectively, and T_{sp} is the sampling period. Thus, the cost function of the output current control

is defined as

$$J_1 = \left| i_{oj}^*(k + 1) - i_{oj}(k + 1) \right| \tag{4}$$

where, i_{oj}^* represents the reference of the output ac-side current.

B. CIRCULATING CURRENT CONTROL

The second control objective is the suppression of circulating currents, which are generated due to the unbalanced voltages in the upper and lower arms of the phase leg. The mathematical equation that describes the model of the circulating current from Fig. 1 is expressed as

$$i_{circj} = \frac{1}{2}(i_{uj} + i_{lj}) - \frac{1}{3}I_{dc} \tag{5}$$

$$\frac{di_{circj}}{dt} = \left(\frac{1}{2L_a} \right) (V_{dc} - (v_{uj} + v_{lj})) \tag{6}$$

In a similar way to the output current control, by using Euler approximation for the circulating current derivative, the mathematical model of the circulating current can be presented as

$$i_{circj}(k + 1) = \left(\frac{T_{sp}}{2L_a} \right) (V_{dc} - (v_{uj}(k) + v_{lj}(k))) + i_{circj}(k) \tag{7}$$

Thus, the cost function of the circulating current is defined as

$$J_2 = \left| i_{circj}^*(k + 1) - i_{circj}(k + 1) \right| \tag{8}$$

where, $i_{circj}(k + 1)$ and $i_{circj}^*(k + 1)$ are the predicted circulating current and reference of circulating current, respectively.

C. ARM ENERGY BALANCING CONTROL

The energy balancing control objective allows the energy of each arm to remain at the reference value, as well as ensure the proper steady-state operation of the MMC. Assuming that the capacitor voltages are kept at the reference value of V_{dc}/N , then the voltages in the upper and the lower arms of phase- j can be described, respectively, as

$$v_{uj} = \frac{n_{uj}}{N} \sum_{m=1}^N v_{Cumj} \tag{9}$$

$$v_{lj} = \frac{n_{lj}}{N} \sum_{m=1}^N v_{Cmj} \tag{10}$$

where, n_{uj} and n_{lj} are the number of the inserted SMs in the upper and lower arms, respectively; and v_{Cumj} and v_{Cmj} are the individual SM capacitor voltages of upper and lower arms, respectively. Therefore, the predicted sum of the SM capacitor voltages in the upper and lower arms becomes:

$$\sum v_{Cuj}(k + 1) = n_{uj}i_{uj}(k) \frac{T_{sp}}{C} + \sum_{m=1}^N v_{Cumj}(k) \tag{11}$$

$$\sum v_{Clj}(k + 1) = n_{lj}i_{lj}(k) \frac{T_{sp}}{C} + \sum_{m=1}^N v_{Cmj}(k) \tag{12}$$

The predicted energy of the upper and lower arms, $W_{uj}(k + 1)$ and $W_{lj}(k + 1)$, are expressed mathematically as

$$W_{uj}(k + 1) = \frac{C}{2N} \left(\sum v_{Cumj}(k + 1) \right)^2 \quad (13)$$

$$W_{lj}(k + 1) = \frac{C}{2N} \left(\sum v_{Clmj}(k + 1) \right)^2 \quad (14)$$

As mentioned previously, the reference value of the SM capacitor voltage is V_{dc}/N in steady-state operation, thus the reference value of the energy of each arm can be presented as

$$W_{uj}^* = W_{lj}^* = \frac{C}{2N} V_{dc}^2 \quad (15)$$

Then, the cost function of the arm energy balancing control is defined as

$$J_3 = \left| W_{uj}(k + 1) - W_{uj}^* \right| + \left| W_{lj}(k + 1) - W_{lj}^* \right| \quad (16)$$

With the three control objectives analyzed previously, combining equation (4), (8), and (16), the cost function of the proposed MPC strategy is defined as

$$J = \lambda_1 J_1 + \lambda_2 J_2 + \lambda_3 J_3 \quad (17)$$

where, λ_1 , λ_2 and λ_3 are weighting factors of the corresponding subsection of cost function.

The weighting factor of the output current λ_1 is set to 1. In addition, the weighting factors λ_2 and λ_3 are determined by an iterative approach with repeated process by updating values. The weighting factor λ_2 is adjusted to identify an optimal value to minimize the THD values of the output currents and the rms values of the circulating currents, whereas the weighting factor λ_3 was set to zero. A value of λ_2 resulting in optimal performances in terms of the THD values of the output currents and the rms values of the circulating currents was selected. Next, regarding the weighting factor λ_3 , the deviation of average capacitor voltages D from the nominal voltage V_{dc}/N , defined by (18), was tested according to different values of the weighting factor λ_3 , with the weighing factor λ_2 obtained in the previous process, to find an optimal value for the weighting factor λ_3 , to keep the average SM capacitor voltages as closest as to the nominal voltage V_{dc}/N . After determining an optimal value for the weighting factor λ_3 , the same procedure to achieve the optimal value for λ_2 , to minimize the THD values of the output currents and the rms values of the circulating currents, is repeated to update an optimal value λ_2 . With the updated λ_2 , the same process to find an optimal λ_3 with the new λ_2 , is conducted repeatedly to determine a new optimal value for λ_3 . This process was repeated by 30 times to find optimal values for the weighting factors.

$$D = \frac{\sum_{m=1}^N \left| v_{Cumj} - V_{dc}/N \right| + \sum_{m=1}^N \left| v_{Culj} - V_{dc}/N \right|}{2N} \quad (18)$$

Fig. 4 illustrates the THD values of the output currents and the rms values of the circulating currents versus varying λ_2 , and $\lambda_1 = 1$, and $\lambda_3 = 10^{-5}$. It can be concluded that the optimum

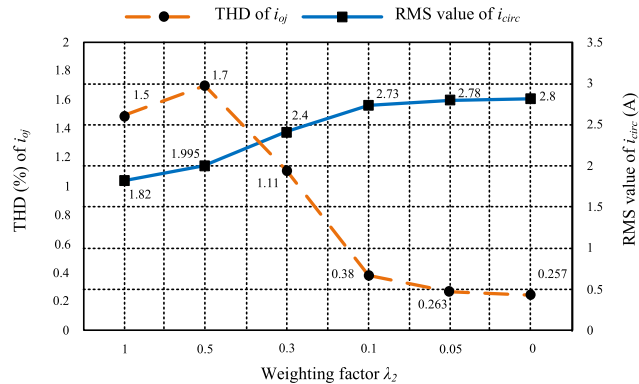


FIGURE 4. THD values of output currents and rms values of circulating currents versus varying λ_2 ($\lambda_1 = 1$ and $\lambda_3 = 10^{-5}$).

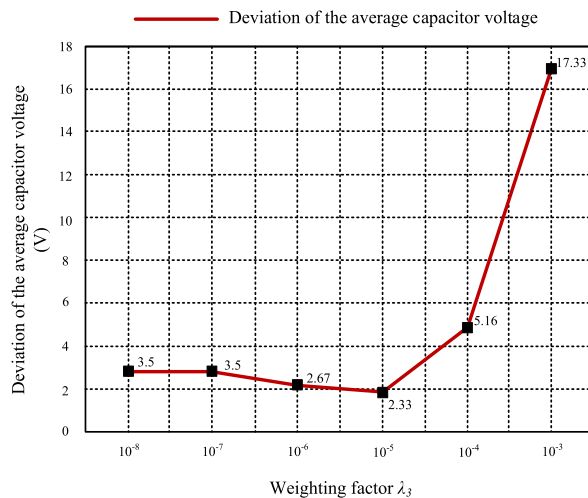


FIGURE 5. Deviation of average capacitor voltages from the nominal voltage dependent on values of weighting factor λ_3 ($\lambda_1 = 1$ and $\lambda_2 = 0.05$).

performance in terms of the THD values of the output currents and the rms values of the circulating currents occurs with $\lambda_2 = 0.05$, which was selected in this paper. Fig. 5 depicts the deviation of average capacitor voltages from the nominal voltage V_{dc}/N , defined by (18), dependent on values of the weighting factor λ_3 . It is seen that the deviation of average capacitor voltages from the nominal voltage is smallest with $\lambda_3 = 10^{-5}$ which was selected in this paper.

Fig. 6 illustrates the flow chart of the proposed method. The relationship between the number of control option $N_{control_option}$ and the number of SM N is shown in Table 1.

D. PRESELECT NUMBER OF INSERTED SMs STRATEGY

By using equations (6) and (7), the circulating currents of the MMC are derived by the upper and lower arm voltages. In balanced MMC capacitor voltage condition, the arm voltage can be expressed as

$$v_{uj} = n_{uj} v_{Cuavg} \quad (19)$$

$$v_{lj} = n_{lj} v_{Clavg} \quad (20)$$

$$v_{Cuavg} = v_{Clavg} = \frac{V_{dc}}{N} \quad (21)$$

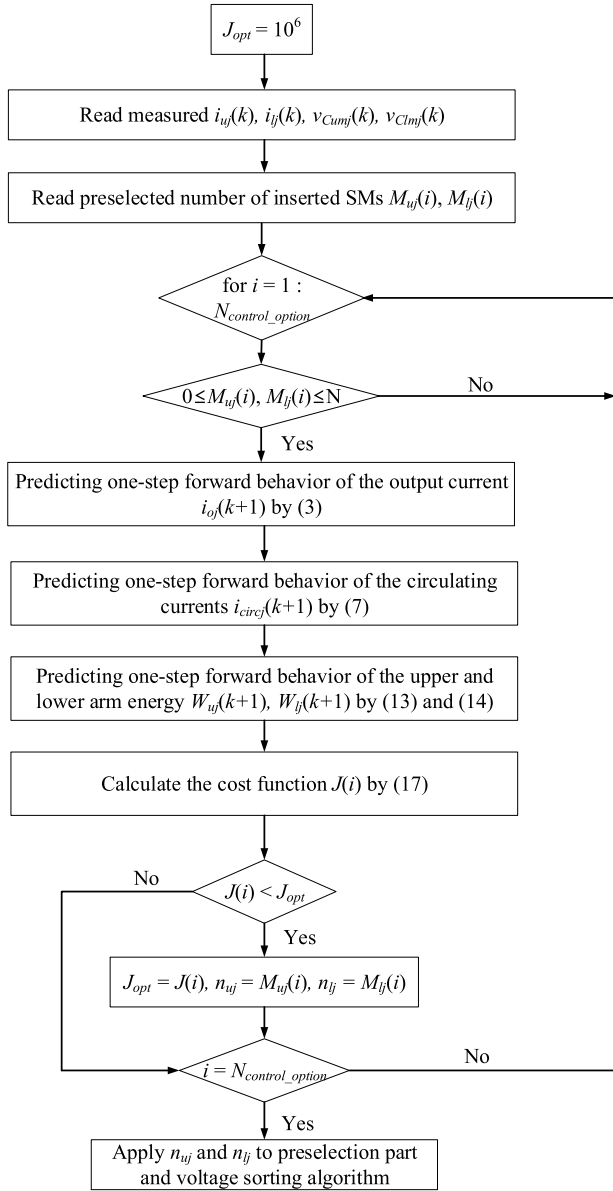


FIGURE 6. Flow chart of proposed method.

where, v_{Cuavg} and v_{Clavg} are the average upper and lower arm capacitor voltages, respectively. By using equations (19), (20) and (21), equation (7) can be expressed as

$$i_{circj}(k+1) = \left(\frac{T_{sp}}{2L_a} \right) \left(V_{dc} - \frac{V_{dc}}{N} (n_{uj} + n_{lj}) \right) + i_{circj}(k) \quad (22)$$

where, $s_j = n_{uj} + n_{lj}$ is the number of on-state SMs in one phase. As mentioned above, in $2N + 1$ output voltage level MMCs, the number of on-state SMs in one phase can equal $N - \alpha, N - \alpha + 1, N - \alpha + 2, \dots, N, N + 1, N + 2, \dots,$ and $N + \alpha$ ($1 \leq \alpha \leq N$). On the contrary, the first term in equation (7), being conditional on its sign, is in charge of the rise or fall of the circulating currents in the next sampling instant $k + 1$. It means that if $s_j > N$, the circulating current in the next sampling instant $k + 1$ tends to decrease, while it

increases if $s_j < N$. Moreover, from [2], in $2N + 1$ output voltage level MMCs, the number of on-state SMs $N + \alpha$ and $N - \alpha$ generate the same output voltage level. Thus, the number of on-state SMs $N + \alpha$ and $N - \alpha$ have an opposite effect on the circulating currents. Furthermore, to reduce the computation load when generating the $2N + 1$ output voltage level and controlling the circulating current, α will be limited. The principle for selecting α , which allows a guarantee of the circulating current controllability with regard to the number of SMs, is given in the Appendix of [20]. It points out that $\alpha = 1$ can be utilized with a low number of SMs ($N < 13$).

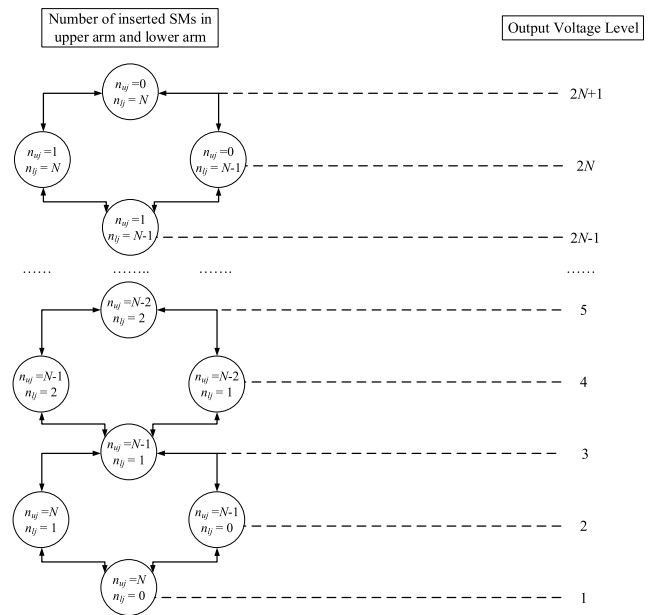


FIGURE 7. Relationship between the output voltage level and the number of inserted SMs in the upper and lower arm.

From the above analysis, as the number of on-state SMs is dependent on the circulating currents, the behavior of the circulating currents can be utilized for choosing a proper number of SMs inserted at the next sampling instant. As a result, an adequate number of on-state SMs at the future step can be preselected on the basis of the circulating currents and the nearest output voltage level around the previous one. In this study, only three cases of the number of on-state SMs in one phase ($N, N + 1$, and $N - 1$) are considered, for a low number of N , that can ensure controllability of circulating currents in MMCs while being capable of generating $2N + 1$ output voltage levels. Fig. 7 depicts the relationship between the output voltage levels and the number of SMs inserted in the upper and the lower arms at s_j is equal to $N + 1, N$, and $N - 1$. It is observed that the output voltage level (l_j) can be expressed by

$$l_j = n_{lj} - n_{uj} + N + 1 \quad (23)$$

which starts at $l_j = 1$ with regard to the number of on-state SMs $s_j = n_{uj} + n_{lj} = N$, then $l_j = 2$ with regard to the

number of on-state SMs $s_j = N + 1$ or $s_j = N - 1$, then $l_j = 3$, $s_j = N$, consecutively.

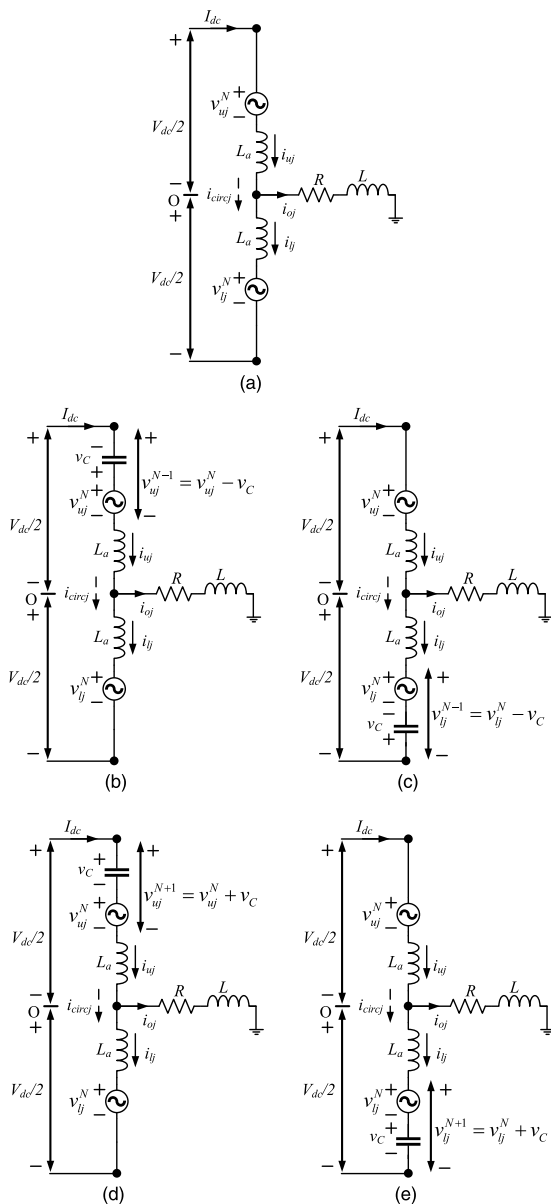


FIGURE 8. One-phase equivalent circuit of the MMC with (a) N on-state SMs (b) $N - 1$ on-state SMs with additional SM capacitor connected to the upper arm (c) $N - 1$ on-state SMs with additional SM capacitor connected to the lower arm (d) $N + 1$ on-state SMs with additional SM capacitor connected to the upper arm (e) $N + 1$ on-state SMs with additional SM capacitor connected to the lower arm.

Fig. 8 (a) illustrates the one-phase equivalent circuit of the MMC with N on-state SMs, where v_{uj}^N and v_{lj}^N is the upper and the lower arm voltage with N on-state SMs, respectively.

The circulating current with N on-state SMs can be expressed as

$$i_{circj}^N(k+1) = \left(\frac{T_{sp}}{2L_a}\right) (V_{dc} - (v_{uj}^N(k) + v_{lj}^N(k))) + i_{circj}(k) \quad (24)$$

In addition, the one-phase equivalent circuit of the MMC with $N - 1$ on-state SMs is shown in Figs. 8 (b) and (c), in which

v_{uj}^{N-1} and v_{lj}^{N-1} is the upper and the lower arm voltage with $N - 1$ on-state SMs, respectively. The arm voltage v_{uj}^{N-1} and v_{lj}^{N-1} can be expressed with one SM capacitor voltage v_c along with the arm voltage v_{uj}^N and v_{lj}^N , respectively, as shown in Figs. 8 (b) and (c). The additional SM capacitor voltage v_c can be located in the upper arm or the lower arm as depicted in Fig. 8 (b) and (c). Because the additional SM capacitor voltage v_c is added in case of the MMC with the $N - 1$ on-state SMs, the circulating current with $N - 1$ on-state SMs is

$$i_{circj}^{N-1}(k+1) = \left(\frac{T_{sp}}{2L_a}\right) (V_{dc} - (v_{uj}^N(k) + v_{lj}^N(k) - v_c)) + i_{circj}(k) \quad (25)$$

Based on (25), it can be known that the circulating current at the $(k + 1)^{th}$ instant, in the case of the MMC with $N - 1$ on-state SMs, is increased compared with the circulating current at the k^{th} instant. On the other hand, Figs. 8 (d) and (e) illustrate the one-phase equivalent circuit of the MMC with $N + 1$ on-state SMs, in which v_{uj}^{N+1} and v_{lj}^{N+1} are the upper and the lower arm voltage with $N + 1$ on-state SMs, respectively. The arm voltage v_{uj}^{N+1} and v_{lj}^{N+1} can be related with one SM capacitor voltage v_c along with the arm voltage v_{uj}^N and v_{lj}^N , respectively, as shown in Figs. 8 (d) and (e). The additional SM capacitor voltage v_c can be located in the upper arm or the lower arm as depicted in Figs. 8 (d) and (e). Note that the polarity of the additional SM capacitor voltage is opposite to the $N - 1$ on-state SM case. Because the additional SM capacitor voltage v_c is added in case of the MMC with the $N + 1$ on-state SMs, the circulating current with $N + 1$ on-state SMs is

$$i_{circj}^{N+1}(k+1) = \left(\frac{T_{sp}}{2L_a}\right) (V_{dc} - (v_{uj}^N(k) + v_{lj}^N(k) + v_c)) + i_{circj}(k) \quad (26)$$

Thus, it can be seen from (26) that, in the case of the MMC with $N + 1$ on-state SMs, the circulating current at the next sampling instant is lower than the circulating current at the present instant.

Based on the aforementioned analysis, the preselection number of inserted SMs algorithm for a low number of SMs is constructed, which is depicted in Fig. 9. The preselection algorithm analyzes s_j , circulating current $i_{circj}(k)$, and the reference circulating current i_{circj}^* , based on the behavior of the circulating currents and considers the three possible numbers of on-state SMs ($N - 1$, N , and $N + 1$) to predict the number of inserted SMs. This will correspond to the nearest output voltage level around the previous output voltage level at the sampling instant k to be evaluated in the next sampling instant $k + 1$.

For instance, an example is visualized by Fig. 10 in the case of the number of SMs $N = 5$. Numbers in Fig. 10 represent all the possibilities of the number of inserted SMs in the upper and lower arms, corresponding to all of the number of on-state SMs cases from 0 to $2N$. The gray part represents

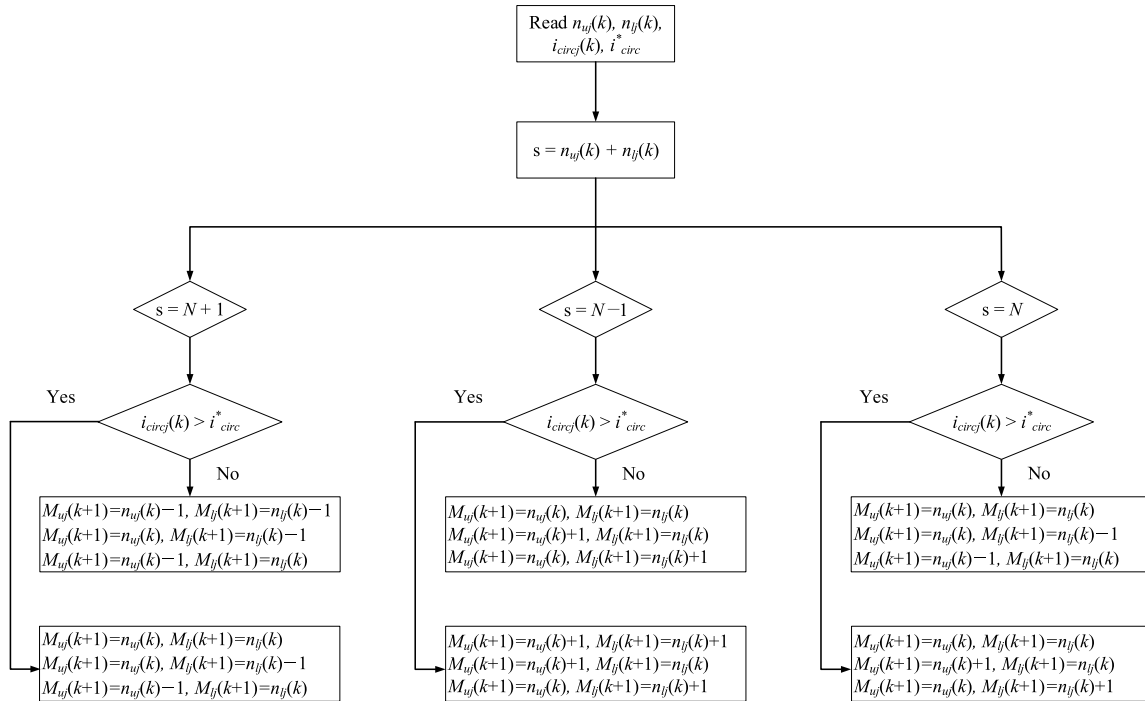


FIGURE 9. Proposed preselected number of inserted SMs algorithm.

the possibility of the number of inserted SMs, corresponding to the number of on-state SMs cases N , $N - 1$ and $N + 1$. The black dashed line and red dashed line represent the preselection algorithm at two cases $i_{circj} > i_{circ}^*$ and $i_{circj} < i_{circ}^*$, respectively. If the controller applied $n_{uj} = 2$, $n_{lj} = 3$ ($s_j = n_{uj} + n_{lj} = 5 = N$, output voltage level $l_j = 7$) in the sampling instant k , in the case of $i_{circj} > i_{circ}^*$, the preselected number of inserted SMs will be generated by the original $M_{uj} = n_{uj} = 2$, $M_{lj} = n_{lj} = 3$; $M_{uj} = n_{uj} + 1 = 3$, $M_{lj} = n_{lj} = 3$ ($s_j = 6 = N + 1$, $l_j = 6$), and $M_{uj} = n_{uj} = 2$, $M_{lj} = n_{lj} + 1 = 4$ ($s_j = 6 = N + 1$, $l_j = 8$) as illustrated in Fig. 9. The preselected number of inserted SMs generate the output voltage $l_j = 6$ and $l_j = 8$ around the previous output voltage level $l_j = 7$ which resulted in a low dv/dt in the output voltage. In other cases, the same process is used, as illustrated in Fig. 9. Furthermore, because there are some cases of preselected number of inserted SMs that can be negative or exceed N (which are not logical), the MPC algorithm in Fig. 6 eliminates those cases.

E. VOLTAGE SORTING ALGORITHM

In this paper, the voltage sorting algorithm in [15] is utilized to maintain all the capacitor voltages of the MMC in balance. This reads the number of SMs n_{uj} and n_{lj} for the upper and lower arms, respectively (to be inserted), the direction of the arm currents i_{uj} , i_{lj} and the magnitude of the capacitor voltages v_{Cumj} , v_{Clmj} are considered to decide which SMs to connect or bypass, as depicted in Fig. 11. Then, the switching states S_{xj} are generated to send to the MMC, which are applied at sampling instant k .

0-0	0-1	0-2	0-3	0-4	0-5
1-0	1-1	1-2	1-3	1-4	1-5
2-0	2-1	2-2	2-3	2-4	2-5
3-0	3-1	3-2	3-3	3-4	3-5
4-0	4-1	4-2	4-3	4-4	4-5
5-0	5-1	5-2	5-3	5-4	5-5

FIGURE 10. Visualization of the preselection algorithm with $N = 5$.

F. EXTENSION OF THE PROPOSED METHOD

The higher number of submodules, the more computational load problem which is solved by the proposed method, but there exists an issue corresponding to the controllability of the circulating current. Its deviation will be large as the number of submodules increases, and this exerts a huge negative impact on the balance of the capacitor voltages [21]. In this case, the preselection algorithm can be operated to ensure the circulating current controllability, by extending the limit of α . As mentioned above, following the principle of α selection in Appendix in [20], α should be at least 7.5% of the number of SMs N , to guarantee minimization of the circulating current.

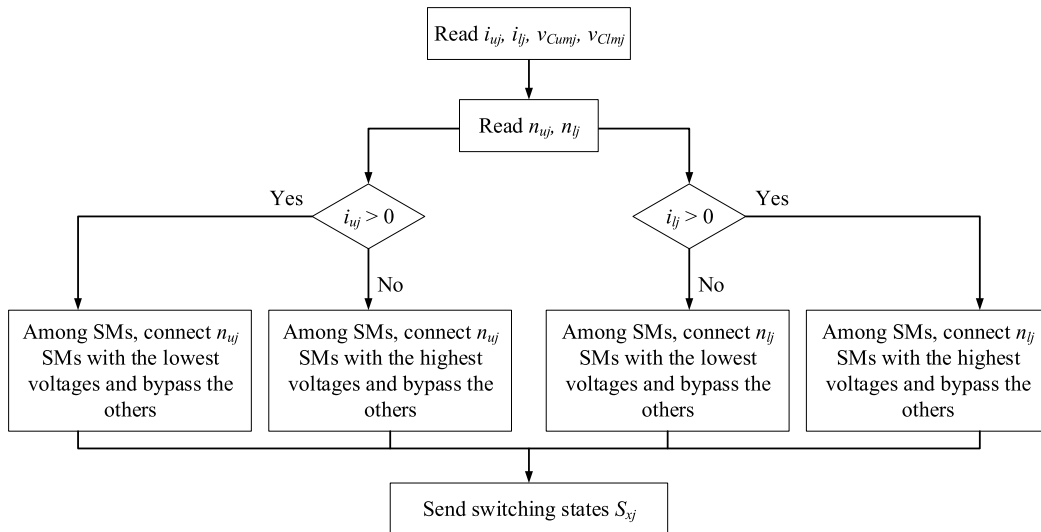


FIGURE 11. Capacitor voltage sorting algorithm.

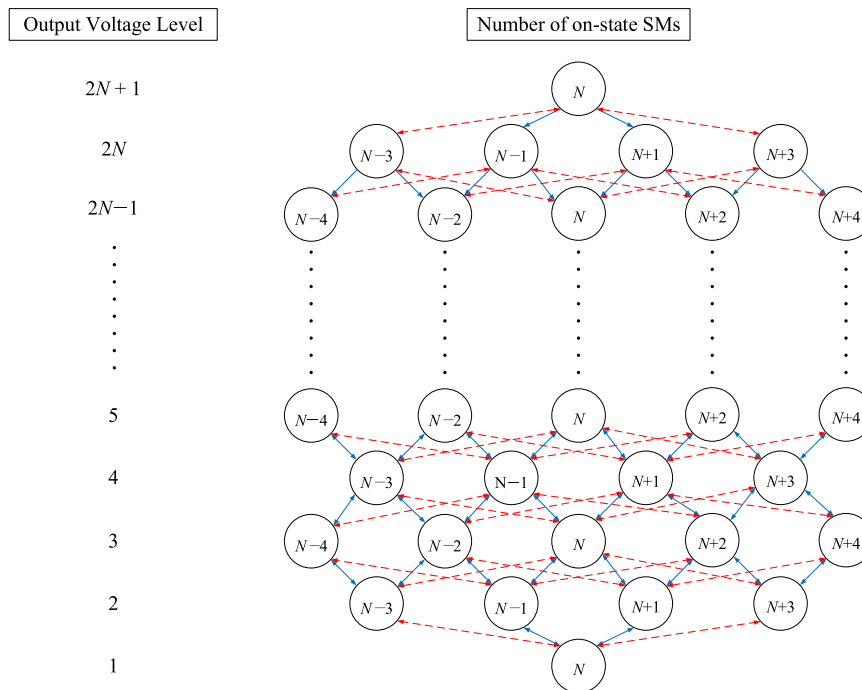


FIGURE 12. Relationship between additional number of on-state SMs in one phase and output voltage level.

Fig. 12 depicts the correlation of the output voltage levels and additional number of on-state SMs in one phase, in the case of $\alpha = 4$. These are capable of being used for all output voltage levels of the MMC, except the lowest and the highest. The additional number of on-state SMs in one phase changes the number of inserted SMs but does not affect the sufficient of the output voltage level. Using the additional number of on-state SMs, the number of control options of the proposed MPC method increases in proportion to the number of SMs as in Table 1.

The proposed method utilizes the preselection algorithm, which preselects the number of inserted SMs in the upper and lower arms. The preselected number of inserted SMs, which is generated based on the relationship between the number of on-state SMs and the circulating current, corresponds to the output voltage level in the previous sampling instant to evaluate in the next sampling instant. The proposed method can reduce computational burden of MMCs by decreasing the number of control options every sampling instant. In particular, as for a large number of SMs, the proposed method

TABLE 1. Number of control options among proposed method and previous approaches (in one phase) for generating $2N + 1$ output voltage levels.

Number of SM (N)		2	4	10	20	50	100	200
Number of control option ($N_{control_option}$)	FCS-MPC [11]	16	256	$1.0e^6$	$1.1e^{12}$	$1.3e^{30}$	$1.6e^{60}$	$2.6e^{120}$
	Reduced MPC1 [12]	10	24	114	424	2554	10104	40204
	Reduced MPC2 [12]	18	32	74	144	354	704	1404
	Indirect FCS-MPC [13]	9	25	121	441	2601	10201	40401
	Preselect method [20]	5	5	5	8	13	16	47
	Proposed method	3	3	3	5	8	14	24

can guarantee the controllability of the circulating current by increasing the number of control option.

IV. SIMULATION RESULTS

To verify the performance of the proposed method, the simulation of 3-phase MMC with $N = 7$ were implemented using PSIM software using the system parameters given in Table 2. In the simulation study, the control block diagram of the proposed method is shown in Fig. 3.

TABLE 2. Parameters of MMC system.

Parameter	Simulation	Experiment
DC-link voltage V_{dc} (V)	7000	100
SMs per arm N	7	3
SM capacitor voltage V_c (V)	1000	33.3
SM capacitance C (μ F)	2200	2200
Arm Inductance L_a (mH)	4	4
Load Inductance L (mH)	10	10
Load Resistance R (Ω)	20	20
Output Frequency f_o (Hz)	60	60
Rated MMC kVA S (kVA)	700	0.1
Sampling frequency f_{sp} (kHz)	10	10

A. STEADY-STATE RESULTS

Fig. 13 illustrates the steady-state simulation results of the proposed method, considering a total simulation time of 0.5s. The 3-phase output currents of the proposed method are depicted, verify that the output currents track its reference value, through utilization of the defined cost function, with THD = 0.9%. Fig. 13 monitors the MMC output voltage waveforms, which are 15-level output voltage waveform varying from $-V_{dc}/2$ to $V_{dc}/2$ with $N = 7$. The circulating currents are minimized. The SMs capacitor voltages of the MMC remained in balance, as expected. The capacitor ripple voltages did not exceed 4% of the reference capacitor voltage value V_{dc}/N . The average switching frequency of the simulation conducted with the parameters in Table 2

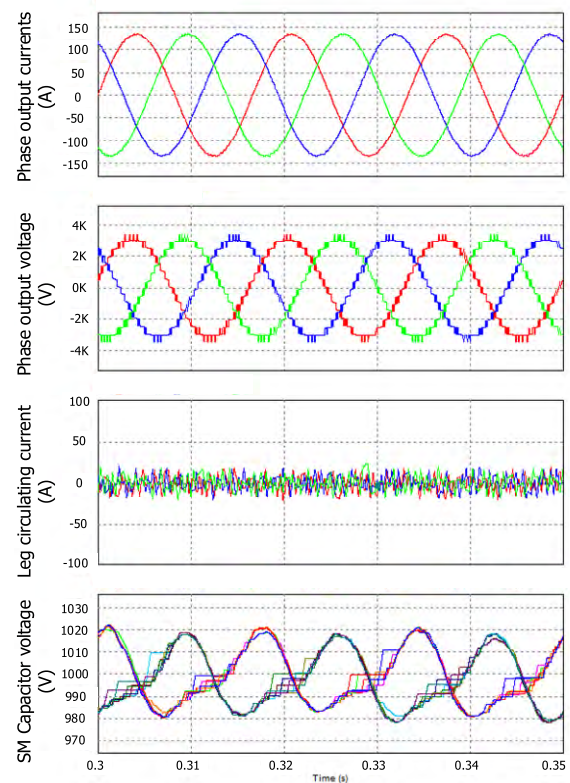


FIGURE 13. Simulation waveforms of phase output currents, phase output voltage, SM capacitor voltages, and circulating currents obtained by 15-level MMC ($N = 7$) at steady state operation operated by proposed method.

was 1427 Hz. The average switching frequency of the MMC operated by the proposed method can be reduced by directly applying the previous approaches to decrease the number of switching in the indirect MPC methods [17], [22], although the reduction scheme of the number of switching was not included in this paper. The steady-state simulation results verify that the proposed method operates correctly and is able to guarantee the control objectives of sinusoidal output

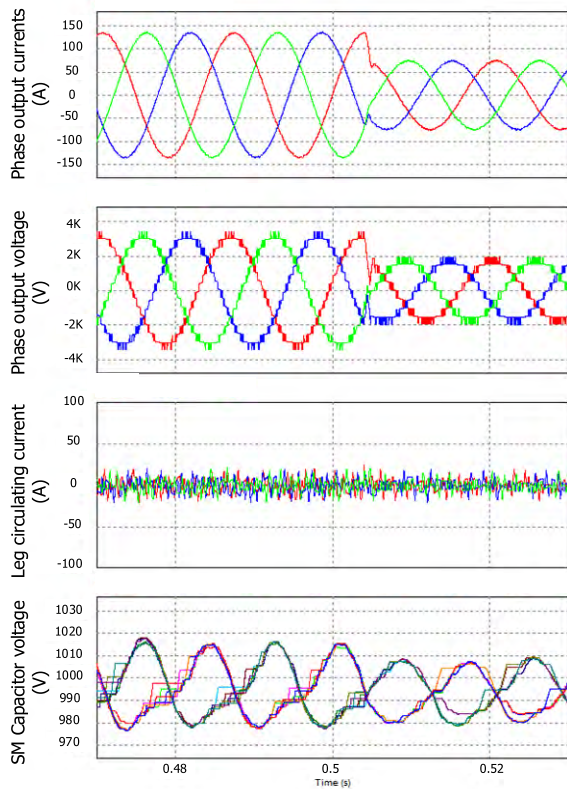


FIGURE 14. Simulation waveforms of phase output currents, phase output voltage, SM capacitor voltages, and circulating currents obtained by 15-level MMC ($N = 7$) at dynamic response operation operated by proposed method with phase output current reference from 135 A to 75 A.

current, minimization of circulating current, and balancing of the SMs capacitor voltage.

B. DYNAMIC PERFORMANCE

The dynamic performance of the proposed method is illustrated in Fig. 14. The MMC was initially controlled to supply a current of 135A to the load. At $t = 0.55s$, the magnitude of the reference output current was decreased from 135A to 75A. The output current of the proposed method correctly tracked a sinusoidal form as well as the magnitude. The output voltages waveform as depicted in Fig. 14, the output voltage level reduces from 15 to 9, while the circulating currents continued to be minimized. The SM capacitor voltages remain balanced at the reference value of V_{dc}/N , with a reduced voltage fluctuation because of the reduction of the reference output current. Accordingly, the dynamic performance of the MMC verified the proper operation of the proposed method.

The effect of the additional number of on-state SMs is depicted in Fig. 15 by simulating for a 41-level MMC ($N = 20$), considering $N, N + 1, N - 1, N + 2, N - 2$ cases. The simulation was implemented by using the same parameter in Table 1, except the increased number of submodule ($N = 20$) and correspondingly increased SM capacitor voltages ($V_C = 350V$) as observed in Fig. 15. Although the

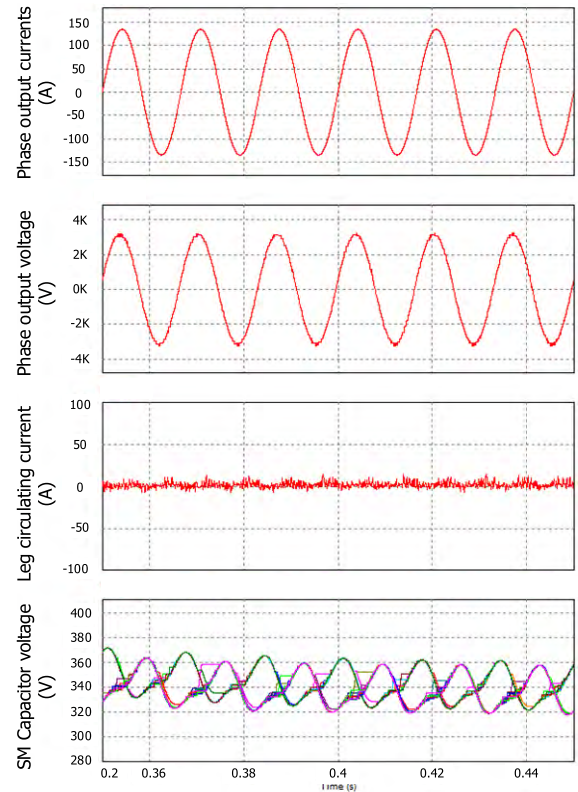


FIGURE 15. Simulation waveforms of phase output current, phase output voltage, circulating current, and SM capacitor voltages obtained by 41-level MMC ($N = 20$) at steady state operation operated by proposed method.

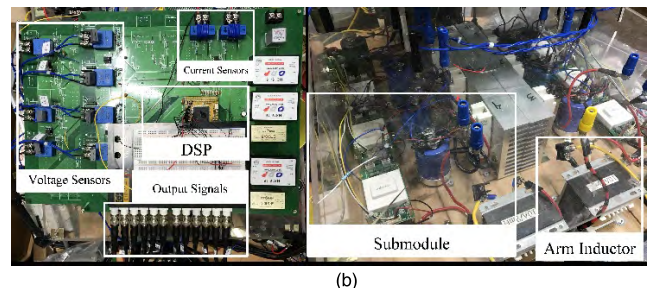
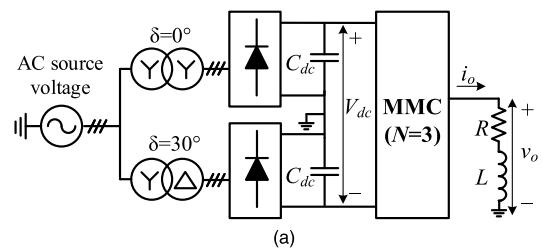


FIGURE 16. Experiment setup of the single-phase MMC (a) Circuit diagram of the experiment setup (b) Single-phase prototype and Control board.

number of SMs is larger ($N = 20$), by applying an additional two more on-state SMs, all control objectives of the MMC is guaranteed such as sinusoidal form of the output current, suppressed circulating current and balance of SM capacitor voltages. The number of control options increased to five,

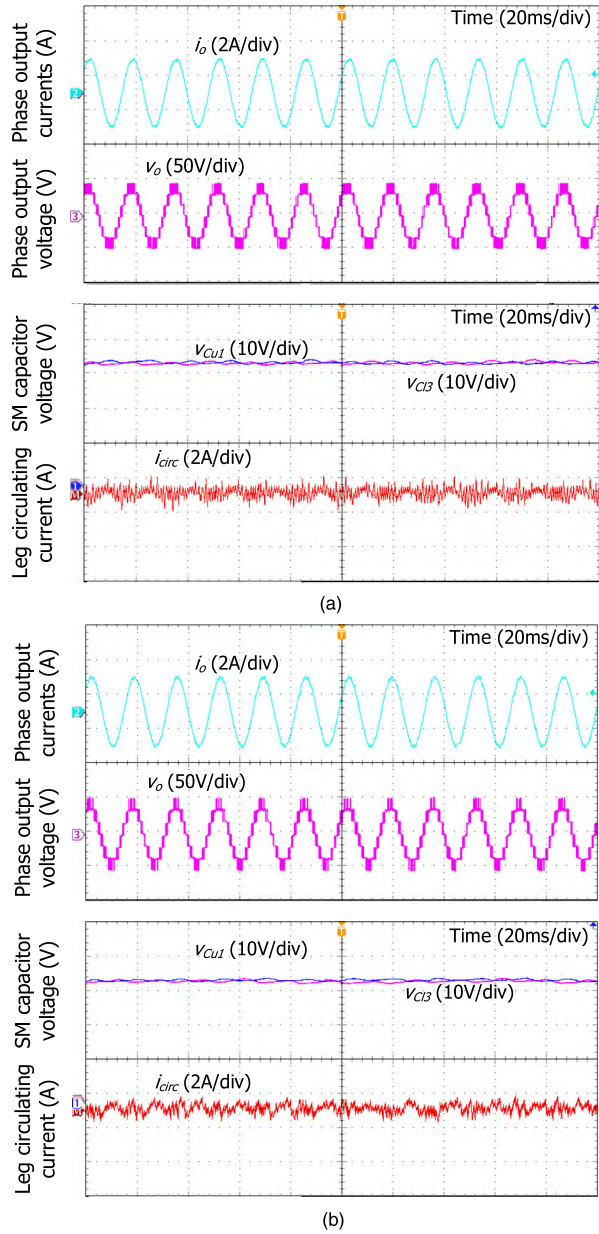


FIGURE 17. Experiment waveforms of MMC ($N = 3$) during steady-state, obtained by (a) proposed method (b) indirect FCS-MPC method.

however, compared to other MPC methods used in Table 1, the number of control options of the proposed method, still to be smaller to reduce the computational load as well as the complexity of the MPC algorithm.

V. EXPERIMENT RESULTS

The performance of the proposed MPC strategy was validated on a single-phase MMC laboratory prototype. The MMC laboratory prototype depicted in Fig. 16 was designed with the system parameters given in Table 1. Each arm comprised three half-bridge submodules that generated seven levels of output voltage. The MMC was controlled by implementing software on a digital signal processor (DSP) board (TMS320F28335), which received the arm current signal of

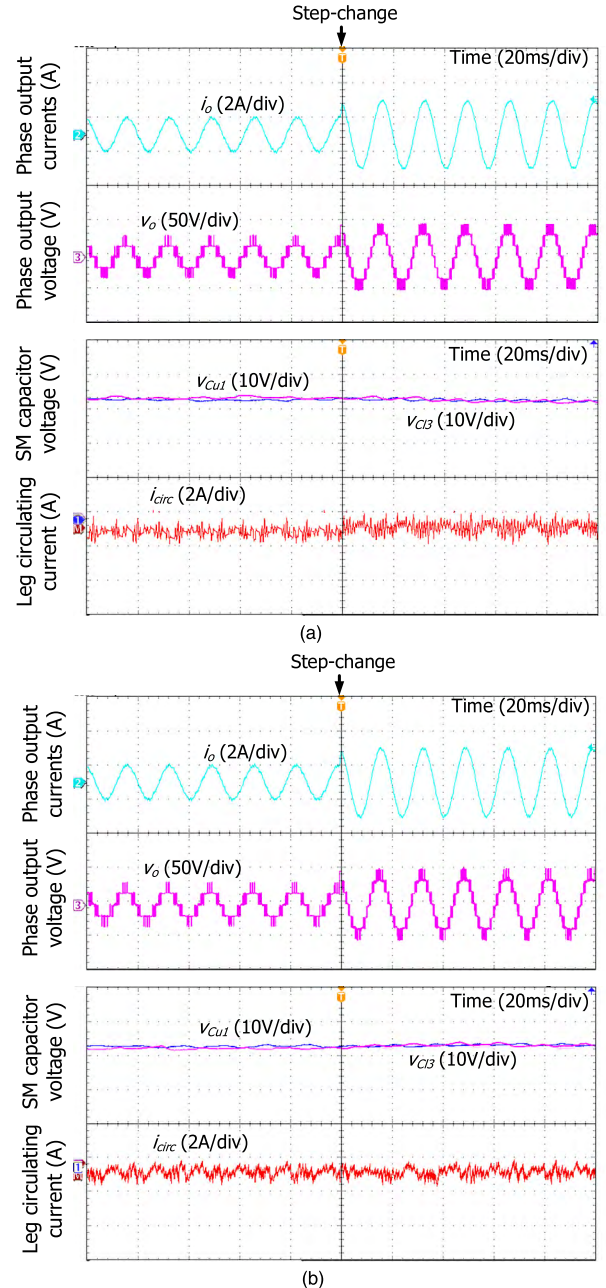


FIGURE 18. Experiment waveform of MMC ($N = 3$) during transient state with step-change of output reference current from 1A to 2A, obtained by (a) proposed method (b) indirect FCS-MPC method.

the current sensors and the SM capacitor voltages signals of the voltage sensors. Then, it transmitted the switching state signals to the MMC, as observed in Fig. 16. The delay compensation method presented in [19] is utilized in this experiment to ensure the proper implementation of the proposed MPC approach.

As seen from Fig. 17, both the methods lead to almost same steady state performance, where they synthesize sinusoidal output current waveforms with low total harmonic distortion (THD) with 1.72 % and 1.9 % for the proposed and the indirect FCS-MPC methods, respectively. Furthermore, the

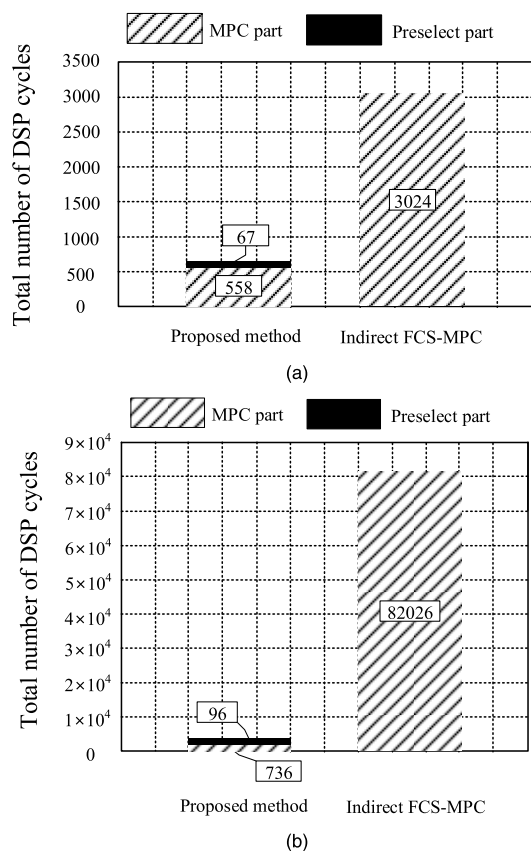


FIGURE 19. Number of DSP cycles compared between the proposed method and indirect FCS-MPC at (a) $N = 3$ and (b) $N = 20$ every sampling instant.

output voltage waveforms generated by both the schemes contain 7-level waveforms varying from $-V_{dc}/2$ to $V_{dc}/2$. In addition, the circulating currents are well suppressed and the SM capacitor voltages are properly balanced for the two algorithms. It can be shown that the circulating current of the proposed method is a little bigger than that of the indirect FCS-MPC method, because of the reduced number of control options of the proposed method in comparison with the indirect FCS-MPC method. The average switching frequency of the experiment operated by the proposed method was 1920 Hz. This verifies that the proposed method is operated correctly.

Fig. 18 shows the experimental waveforms of the MMC ($N = 3$) during transient state with a step-change of the output reference current from 1 A to 2 A, obtained by the proposed method and the indirect FCS-MPC method. It is seen that both the methods yield almost the same dynamic performance, in which the output currents resulted from both the two methods track their references with fast dynamic speed. In addition, the output voltage levels of the two methods are increased from five to seven, according to the step-change. As a result, it can be concluded, in comparison with the indirect FCS-MPC method, that the proposed approach can substantially reduce the computational efforts by decreasing the number of control options as shown in Table 1, whereas it can provide almost the same performance of the MMC converter.

The measured DSP cycle at every sampling instant between the proposed method and indirect FCS-MPC [13] are illustrated in Fig. 19. At number of SM, $N = 3$, the proposed method took 558 DSP cycles for the MPC part, and 67 DSP cycles for the preselection algorithm. These measured DSP cycles were equal to $3.72 \mu\text{s}$ and $0.45 \mu\text{s}$, respectively. Meanwhile, indirect FCS-MPC method requires 3024 DSP cycles, corresponding to $20.16 \mu\text{s}$ to find out the optimal number of inserted SMs at each sampling instant. It can be seen that the proposed method allows the total DSP execution time to decrease nearly 79% compared to indirect FCS-MPC at $N = 3$. Furthermore, when the number of SMs increased up to $N = 20$ as shown in Fig. 19 (b), the proposed method allowed a significant reduction of the DSP cycles compared to a conventional indirect FCS-MPC method [13]. The total DSP execution time of the proposed method is 98.98% less than indirect FCS-MPC.

VI. CONCLUSION

This paper proposed the simplified MPC method with the preselection algorithm to determine the number of inserted SMs at the upper and lower arm for the MMC generating the $2N + 1$ output voltage levels. The developed algorithm can reduce the number of control options and correspondingly computation loads, by utilizing the number of on-state SMs in one phase and their effect on the circulating currents. A cost function was designed to select the most suitable number of inserted SMs for each arm to suppress both the output current tracking error and the circulating current as well as to retain the arms energy balancing. The proposed approach substantially improved computational loads of the MPC by reducing the number of control options, ensuring three crucial controlling objectives of the MMC: correction of sinusoidal form, magnitude of output current or voltage, suppression of circulating current inside the converter, and voltage balancing the capacitors of the submodules. Especially, as for the MMC with a large number of SMs, the proposed method can guarantee the circulating current controllability with less complexity, by increasing the number of control options. The performance of the proposed method was verified with simulation and experiment results.

REFERENCES

- [1] M. A. Perez, S. Bernet, J. Rodriguez, S. Kouro, and R. Lizana, "Circuit topologies, modeling, control schemes, and applications of modular multilevel converters," *IEEE Trans. Power Electron.*, vol. 30, no. 1, pp. 4–17, Jan. 2015.
- [2] G. S. Konstantinou, M. Ciobotaru, and V. G. Agelidis, "Analysis of multi-carrier PWM methods for back-to-back HVDC systems based on modular multilevel converters," in *Proc. 37th Annu. Conf. IEEE Ind. Electron. Soc.*, Nov. 2011, pp. 4391–4396.
- [3] M. Hagiwara and H. Akagi, "Control and experiment of pulsewidth-modulated modular multilevel converters," *IEEE Trans. Power Electron.*, vol. 24, no. 7, pp. 1737–1746, Jul. 2009.
- [4] M. Hagiwara, R. Maeda, and H. Akagi, "Control and analysis of the modular multilevel cascade converter based on double-star chopper-cells (MMCC-DSCC)," *IEEE Trans. Power Electron.*, vol. 26, no. 6, pp. 1649–1658, Jun. 2011.
- [5] Z. Li, P. Wang, H. Zhu, Z. Chu, and Y. Li, "An improved pulse width modulation method for chopper-cell-based modular multilevel converters," *IEEE Trans. Power Electron.*, vol. 27, no. 8, pp. 3472–3481, Aug. 2011.

- [6] S. Kouro, P. Cortes, R. Vargas, U. Ammann, and J. Rodriguez, "Model predictive control—A simple and powerful method to control power converters," *IEEE Trans. Ind. Electron.*, vol. 56, no. 6, pp. 1826–1838, Jun. 2009.
- [7] P. Cortes, A. Wilson, S. Kouro, J. Rodriguez, and H. Abu-Rub, "Model predictive control of multilevel cascaded H-bridge inverters," *IEEE Trans. Ind. Electron.*, vol. 57, no. 8, pp. 2691–2699, Aug. 2010.
- [8] L. Guo, X. Zhang, S. Yang, Z. Xie, and R. Cao, "A model predictive control-based common-mode voltage suppression strategy for voltage-source inverter," *IEEE Trans. Ind. Electron.*, vol. 63, no. 10, pp. 6115–6125, Oct. 2016.
- [9] R. N. Fard, H. Nademi, and L. Norum, "Analysis of a modular multilevel inverter under the predicted current control based on finite-control-set strategy," in *Proc. 3rd Int. Conf. Electr. Power Energy Convers. Syst. (EPECS)*, Oct. 2013, pp. 1–6.
- [10] J. Qin and M. Saeedifard, "Predictive control of a modular multilevel converter for a back-to-back HVDC system," *IEEE Trans. Power Del.*, vol. 27, no. 3, pp. 1538–1547, Jul. 2012.
- [11] J. Bocker, B. Freudenberg, A. The, and S. Dieckerhoff, "Experimental comparison of model predictive control and cascaded control of the modular multilevel converter," *IEEE Trans. Power Electron.*, vol. 30, no. 1, pp. 422–430, Jan. 2015.
- [12] J.-W. Moon, J.-S. Gwon, J.-W. Park, D.-W. Kang, and J.-M. Kim, "Model predictive control with a reduced number of considered states in a modular multilevel converter for HVDC system," *IEEE Trans. Power Del.*, vol. 30, no. 2, pp. 608–617, Apr. 2015.
- [13] M. Vatani, B. Bahrani, M. Saeedifard, and M. Hovd, "Indirect finite control set model predictive control of modular multilevel converters," *IEEE Trans. Smart Grid*, vol. 6, no. 3, pp. 1520–1529, May 2015.
- [14] F. Zhang, W. Li, and G. Joós, "A voltage-level-based model predictive control of modular multilevel converter," *IEEE Trans. Ind. Electron.*, vol. 63, no. 8, pp. 5301–5312, Aug. 2016.
- [15] Z. Gong, P. Dai, X. Yuan, X. Wu, and G. Guo, "Design and experimental evaluation of fast model predictive control for modular multilevel converters," *IEEE Trans. Ind. Electron.*, vol. 63, no. 6, pp. 3845–3856, Jun. 2016.
- [16] S. Debnath, J. Qin, B. Bahrani, M. Saeedifard, and P. Barbosa, "Operation, control, and applications of the modular multilevel converter: A review," *IEEE Trans. Power Electron.*, vol. 30, no. 1, pp. 37–53, Jan. 2015.
- [17] P. Liu, Y. Wang, W. Cong, and W. Lei, "Grouping-sorting-optimized model predictive control for modular multilevel converter with reduced computational load," *IEEE Trans. Power Electron.*, vol. 31, no. 3, pp. 1896–1907, May 2016.
- [18] L. Harnefors, A. Antonopoulos, S. Norrga, L. Ångquist, and H.-P. Nee, "Dynamic analysis of modular multilevel converters," *IEEE Trans. Ind. Electron.*, vol. 60, no. 7, pp. 2526–2537, Jul. 2013.
- [19] J. Rodriguez and P. Cortes, *Predictive Control of Power Converters and Electrical Drives*. Hoboken, NJ, USA: Wiley, 2012.
- [20] B. Gutierrez and S.-S. Kwak, "Modular multilevel converters (MMCs) controlled by model predictive control with reduced calculation burden," *IEEE Trans. Power Electron.*, vol. 33, no. 11, pp. 9176–9187, Nov. 2018.
- [21] X. Li, Q. Song, W. Liu, S. Xu, Z. Zhu, and X. Li, "Performance analysis and optimization of circulating current control for modular multilevel converter," *IEEE Trans. Ind. Electron.*, vol. 63, no. 2, pp. 716–727, Feb. 2016.
- [22] Q. Tu, Z. Xu, and L. Xu, "Reduced switching-frequency modulation and circulating current suppression for modular multilevel converters," *IEEE Trans. Power Del.*, vol. 26, no. 3, pp. 2009–2017, Jul. 2011.



MINH HOANG NGUYEN received the B.S. degree in electrical and electronics engineering from the Hanoi University of Science and Technology, Vietnam, in 2016. He is currently pursuing the M.S. and Ph.D. combined degree in electrical and electronics engineering with Chung-Ang University, Seoul, South Korea. His research interests are control and analysis for multilevel converters.



SANGSHIN KWAK (S'02–M'05) received the Ph.D. degree in electrical engineering from Texas A&M University, College Station, TX, USA, in 2005. From 1999 to 2000, he was a Research Engineer with LG Electronics, Changwon, South Korea. He was also with the Whirlpool Research and Development Center, Benton Harbor, MI, USA, in 2004. From 2005 to 2007, he was a Senior Engineer with the Samsung SDI Research and Development Center, Yongin, South Korea. From 2007 to 2010, he was an Assistant Professor with Daegu University, Gyeongsan, South Korea. Since 2010, he has been with Chung-Ang University, Seoul, South Korea, where he is currently a Professor. His research interests are topology design, modeling, modulation, and control of power converters, multilevel converters, renewable energy systems, and power quality.

...